

“Molecular Hysteresis” in an Electrochemical System Revisited

Mitsuru Sano*

Department of Chemistry, College of General Education, Nagoya University, and Presto-21 Project, JRDC, Nagoya 464-01, Japan

Henry Taube

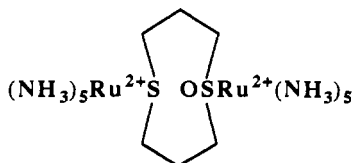
Department of Chemistry, Stanford University, Stanford, California 94305

Received August 28, 1993*

Earlier work on the electrochemical behavior of (1,5-dithiacyclooctane 1-oxide)bis(pentaammineruthenium) has been repeated and extended so that the kinetic and equilibrium parameters which define the “double-block” diagram are now determined (acetone as solvent, 20 °C). The metastable fully oxidized form ($\text{Ru}^{3+}\text{-SO}/\text{Ru}^{3+}\text{-S}$) decays to the stable isomer ($\text{Ru}^{3+}\text{-OS}/\text{Ru}^{3+}\text{-S}$) at a specific rate of 13 s^{-1} ; ΔG° for the reaction is -36 kJ mol^{-1} . The metastable fully reduced form ($\text{Ru}^{2+}\text{-OS}/\text{Ru}^{2+}\text{-S}$) decays to the stable form ($\text{Ru}^{2+}\text{-SO}/\text{Ru}^{2+}\text{-S}$) at a specific rate of 3.8 s^{-1} ; $\Delta G^\circ = -55\text{ kJ mol}^{-1}$. In the mixed-valence state, ($\text{Ru}^{3+}\text{-OS}/\text{Ru}^{2+}\text{-S}$) changes to ($\text{Ru}^{2+}\text{-SO}/\text{Ru}^{3+}\text{-S}$) by intramolecular electron transfer at a specific rate of 0.12 s^{-1} ($\Delta G^\circ = -1.9\text{ kJ mol}^{-1}$). Completion of the evaluation of the dynamic parameters was enabled by the direct determination of those cited for the mixed-valence state.

The prospect of using molecules (or small assemblies of molecules) as elements in electronic circuits is an exciting challenge for chemists. A number of ideas along these lines, for example the application of molecules as switches or memory devices, have been proposed.¹ An important requirement in most applications is that the elements have the capacity to persist in more than one state under the same values of applied external forces: bistable or multistable systems are the key building blocks of all digital electronic devices. Elements which show hysteresis play a special role in applications, particularly in memory devices.²

Hysteresis as it occurs in a collection of interacting particles is a well-known phenomenon, most commonly encountered in the magnetic behavior of some solids. It is not altogether surprising to find it on a “molecular level” in polymers³ such as proteins and nucleic acids which are polysegmented and can adopt higher order structures. In an earlier report⁴ we described the simple molecule



which was designed to exhibit important features of a hysteresis loop. In the species (1,5-dithiacyclooctane 1-oxide)bis(pentaammineruthenium(II)), a reversible couple— $(\text{NH}_3)_5\text{Ru}^{3+/2+}$

ligated to the thioether function⁵—is combined with the couple $\text{Ru}(\text{NH}_3)_5\text{Ru}^{3+/2+}$ bound to the sulfoxide function, a combination which shows linkage isomerization on electron transfer.⁶ Though not the first example⁷ of the kind of electrochemical behavior we reported, ours is the first system designed to display the elements of molecular hysteresis.

When the molecule is fully reduced, that form is stable in which Ru^{2+} is attached to the sulfur of the sulfoxide linkage, ($\text{Ru}^{2+}\text{-SO}/\text{Ru}^{2+}\text{-S}$) back-bonding being favored in this isomer. When, in cyclic voltammetry, the potential is increased, $1e^-$ oxidation takes place first at the thioether linkage, the reversible couple site, producing ($\text{Ru}^{2+}\text{-SO}/\text{Ru}^{3+}\text{-S}$). Upon a further increase in the potential, ($\text{Ru}^{3+}\text{-SO}/\text{Ru}^{3+}\text{-S}$) is the immediate product of the next $1e^-$ oxidation with the sulfur of sulfoxide being bound to Ru^{3+} . The advantage of back-bonding is now lost, and this isomer rearranges rapidly to ($\text{Ru}^{3+}\text{-OS}/\text{Ru}^{3+}\text{-S}$), where Ru^{3+} is attached to the more negative site of the sulfoxide linkage. Upon a decrease in the applied potential ($\text{Ru}^{3+}\text{-OS}/\text{Ru}^{2+}\text{-S}$) is formed, and on upon a further decrease in potential, ($\text{Ru}^{2+}\text{-OS}/\text{Ru}^{2+}\text{-S}$) is first formed, but this is unstable and rapidly rearranges to ($\text{Ru}^{2+}\text{-SO}/\text{Ru}^{2+}\text{-S}$), completing the cycle. The mixed-valence state exists in two forms, one accessible only by oxidation of the stable fully reduced form, and the other, only by reduction of the stable fully oxidized form, and the entire cycle is as depicted in Figure 2. If the possibility of interconversion of the mixed-valence form is introduced, a double-square potential diagram results.

The earlier work was incomplete, and the values of important dynamic parameters were left undetermined. This report describes the results we have obtained in repeating the measurements and in extending and refining them to the point that reasonably accurate values of the kinetic and equilibrium parameters of the double-block electrochemical cycle have been obtained. All of the new experimental work was done at Nagoya University.

- * To whom correspondence should be addressed at Nagoya University.
 • Abstract published in *Advance ACS Abstracts*, January 1, 1994.
 (1) (a) *Molecular Electronic Devices I*; Carter, F. L., Ed.; Marcel Dekkar: New York, 1982. (b) *Molecular Electronic Devices II*; Carter, F. L., Ed.; Marcel Dekkar: New York, 1987. (c) *Molecular Electronics*; Hong, F. T., Ed.; Plenum: New York, 1989. (d) *Molecular Electronics-Science and Technology*; Aviram, A., Ed.; American Institute of Physics: New York, 1991. (e) Aviram, A.; Ratner, M. A. *Chem. Phys. Lett.* **1974**, *29*, 277. (f) Aviram, A. *J. Am. Chem. Soc.* **1988**, *110*, 5687. (g) Farazdel, A.; Dupuis, M.; Clementi, E.; Aviram, A. *J. Am. Chem. Soc.* **1990**, *112*, 4206. (h) Joachim, C.; Launay, J. P. *Chem. Phys.* **1986**, *109*, 93. (i) Hush, N. S.; Wong, A. T.; Bacsikay, G. B.; Reimers, J. R. *J. Am. Chem. Soc.* **1990**, *112*, 4192.
 (2) (a) Kahn, O.; Launay, J. P. *Chemtronics* **1988**, *3*, 140. (b) Bolvin, H.; Kahn, O. *New J. Chem.* **1991**, *15*, 889.
 (3) Neumann, E. *Angew. Chem., Int. Ed. Engl.* **1973**, *12*, 356.
 (4) (a) Sano, M.; Taube, H. *J. Am. Chem. Soc.* **1991**, *113*, 2327. (b) Sano, M. *Kagaku Asahi* **1991**, *51* (9), 34.

- (5) Stein, C. A.; Taube, H. *J. Am. Chem. Soc.* **1978**, *100*, 1635.
 (6) Yeh, A.; Scott, N.; Taube, H. *Inorg. Chem.* **1982**, *21*, 2542.
 (7) Earlier examples are reported in: Evans, D. H. *Chem. Rev.* **1990**, *90*, 739. The earliest apparently is: Nelson, S. F.; Cunkle, G. T.; Evans, D. H.; Haller, K. J.; Kraftery, M.; Kirste, B.; Kurreck, H.; Clark, T. J. *Am. Chem. Soc.* **1985**, *107*, 3829.

Experimental Section

Proton and carbon-13 NMR spectra were recorded on a JEOL J-270 spectrometer and are reported as ppm shifts from acetone- d_6 (2.04 ppm for ^1H and 29.8 ppm for ^{13}C). Coulometry and bulk electrolysis experiments were performed on a PAR Model 173 potentiostat, with a Model 276 interface, which was driven by a PAR Model 175 universal programmer. Cyclic voltammograms and double potential step experiments were performed by a three-electrode system with a gold working electrode (1-mm diameter), a platinum-wire counter electrode, and a gold-wire reference electrode with ferrocene/ferrocenium hexafluorophosphate dissolved in acetone. Cyclic voltammograms at fast scan rates (1.0–100 V s^{-1}) and double potential step experiments were recorded on a Riken Denshi TCFL-8000E transient recorder. All potentials were reported vs the normal hydrogen electrode. The reference electrode was calibrated with the ferrocene/ferrocenium couple ($E = 0.55 \text{ V (NHE)}$) as measured in situ.

First-order isomerization rate constants were determined with the double potential step chronoamperometry method of Schwarz and Shain.⁸ The stepping potentials were chosen as 400 mV positive and negative of $E_{1/2}$. Current ratios, $i_r(T+\tau)/i_f(T)$, were obtained by measuring the currents for t/τ values of 0.2. The kinetic parameters were obtained from the theoretical working curve.⁸

Reagents. The ligand, 1,5-dithiacyclooctane 1-oxide (SO/S), was synthesized by the method of Roush and Musker.⁹ The oxidized Ru compounds were obtained from the reduced forms in bulk electrolysis with platinum wire (0.01 mm). The acetone was purified by vacuum distillation over B_2O_3 . Anhydrous Et_2O and CH_2Cl_2 were purchased from Aldrich and were used without further purification. All solvents were thoroughly deoxygenated by purging with argon, and reactions were carried out under argon atmosphere in a Vacuum/Atmospheres Co. inert-atmosphere dry glovebox.

Preparation of $[\text{Ru}(\text{NH}_3)_5(\text{SO/S})](\text{PF}_6)_2$ (1). (The same number designations will be used for the cations of interest and the salts containing them.) $[\text{Ru}(\text{NH}_3)_5(\text{acetone})](\text{PF}_6)_2$ (100 mg) was dissolved in 5 mL of acetone. This solution was added to 2 mL of acetone solution containing 130 mg of the ligand SOS. The solution rapidly turned pale yellow from red-brown and was stirred for 10 min. The resulting solution was treated with CH_2Cl_2 (5 mL), and the mixture was filtered. The filtrate was treated with Et_2O (20 mL), and the resulting white precipitate was collected by filtration and washed with ether. The solid was redissolved with a small amount of acetone, the solution was filtered, and the filtrate was treated with CH_2Cl_2 . The resulting precipitate was collected and washed with CH_2Cl_2 .

Anal. Calcd for $\text{C}_6\text{H}_{27}\text{F}_{12}\text{N}_5\text{ORuS}_2^{1/2}(\text{CH}_3)_2\text{CO}$: C, 13.45, H, 4.52; N, 10.46. Found: C, 13.31; H, 4.49; N, 10.18. $^1\text{H NMR}$ (acetone- d_6): δ 3.8–3.6 (br, 7H), 3.0–2.9 (m, 4H), 2.61 (br, 12H), 2.0–1.9 (m, 4H).

Preparation of $[\text{Ru}(\text{NH}_3)_5(\text{SOS})\text{Ru}(\text{NH}_3)_5](\text{PF}_6)_4$, $(\text{Ru}^{2+}\text{-SO/Ru}^{2+}\text{-S})(\text{PF}_6)_4$ (2). Eighty-four milligrams of 1 was dissolved in 3 mL of acetone. To this solution was added 2 mL of the acetone solution containing 67 mg of $[\text{Ru}(\text{NH}_3)_5(\text{acetone})](\text{PF}_6)_2$. The solution was stirred for 20 min. The resulting solution was treated with CH_2Cl_2 (1 mL), and the mixture was filtered. The filtrate was treated with CH_2Cl_2 (4 mL), and the resulting precipitate was collected by filtration and washed with CH_2Cl_2 . The solid was redissolved a small amount of acetone, and CH_2Cl_2 was added. The precipitate was collected by filtration and washed with CH_2Cl_2 .

Anal. Calcd for $\text{C}_6\text{H}_{42}\text{F}_{24}\text{N}_{10}\text{O}_2\text{Ru}_2\text{S}_2^{1/2}(\text{CH}_3)_2\text{CO}$: C, 7.86; H, 3.96; N, 12.22. Found: C, 7.35; H, 3.93; N, 11.73. $^1\text{H NMR}$ (acetone- d_6): δ 3.9–3.8 (m, 4H), 3.81 (s, 3H), 3.33 (s, 3H), 2.9–2.7 (m, 4H), 2.55 (s, 12H), 2.47 (s, 12H), 2.1–2.0 (m, 4H).

General Preparation of $[\text{Ru}(\text{NH}_3)_5(\text{sulfoxide})](\text{PF}_6)_2$. In a typical preparation, 100 mg of $[\text{Ru}(\text{NH}_3)_5(\text{acetone})](\text{PF}_6)_2$ was dissolved in 3 mL of acetone. An excess of the desired sulfoxide was added (500 mg), and the solution was stirred for 10 min. The solution was filtered, and the filtrate was treated with CH_2Cl_2 (5 mL). The resulting precipitate was filtered off and washed with CH_2Cl_2 . The solid was redissolved with acetone, and the solution was treated with CH_2Cl_2 (5 mL). The resulting precipitate was filtered off and washed with CH_2Cl_2 and ether.

The compounds are characterized by ^1H and ^{13}C NMR and cyclic voltammetry.

$[\text{Ru}(\text{NH}_3)_5(\text{dimethyl sulfoxide})](\text{PF}_6)_2$: $^1\text{H NMR}$ (acetone- d_6) δ 3.73 (br, 3H), 3.33 (s, 6H), 2.57 (br, 12H); $^{13}\text{C NMR}$ (acetone- d_6) δ 46.2;

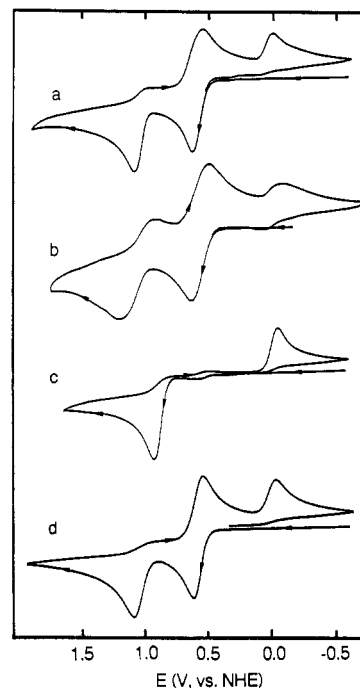


Figure 1. Cyclic voltammograms (in acetone at 20 °C; 0.10 M $(n\text{-Bu})_4\text{PF}_6$ electroactive species at $1.0 \times 10^{-3} \text{ M}$): (a) $[\text{Ru}(\text{NH}_3)_5(\text{SOS})\text{Ru}(\text{NH}_3)_5]^{4+}$ at 100 mV s^{-1} ; (b) $[\text{Ru}(\text{NH}_3)_5(\text{SOS})\text{Ru}(\text{NH}_3)_5]^{4+}$ at 5 V s^{-1} ; (c) $[\text{Ru}(\text{NH}_3)_5(\text{SOS})]^{2+}$ at 100 mV s^{-1} ; (d) digital simulation for $[\text{Ru}(\text{NH}_3)_5(\text{SOS})\text{Ru}(\text{NH}_3)_5]^{4+}$ at 100 mV s^{-1} .

cyclic voltammetry (acetone, 0.10 M $n\text{-Bu}_4\text{NPF}_6$, 100 mV s^{-1}) $E_{\text{pa}} = 1.01 \text{ V}$, $E_{\text{pc}} = -0.01 \text{ V}$.

$[\text{Ru}(\text{NH}_3)_5(\text{diphenyl sulfoxide})](\text{PF}_6)_2$: $^1\text{H NMR}$ (acetone- d_6) δ 7.9–7.8 (m, 4H), 7.6–7.5 (m, 6H), 3.94 (br, 3H), 2.67 (br, 12H); $^{13}\text{C NMR}$ (acetone- d_6) δ 146.9, 132.0, 130.6, 125.9; cyclic voltammetry (acetone, 0.1 M $n\text{-Bu}_4\text{NPF}_6$, 100 mV s^{-1}) $E_{\text{pa}} = 1.11 \text{ V}$, $E_{\text{pc}} = 0.14 \text{ V}$.

Digital Simulations of Cyclic Voltammograms. Digital simulations of proposed electrochemical mechanisms were done with a general-purpose program designed to simulate voltammograms for any mechanism formulated as a combination of heterogeneous charge transfer and homogeneous reactions.¹⁰ The input for the simulations consisted of oxidation–reduction voltages and heterogeneous-charge-transfer rate constants for each electrode process and forward and reverse rate constants for each homogeneous reaction. The transfer coefficients for the heterogeneous charge transfers were assumed to be 0.5.

Results

Overview of the Electrochemistry of $(\text{Ru}^{2+}\text{-SO/Ru}^{2+}\text{-S})$.

Figure 1a shows the trace generated in cyclic voltammetry at a sweep rate of 100 mV s^{-1} for the fully reduced form ($\text{Ru}^{2+}\text{-SO/Ru}^{2+}\text{-S}$). In Figure 1b, the sweep rate is 5 V s^{-1} ; this is sufficiently high that E_{pc}^2 , corresponding to the reduction of the unstable, fully oxidized form ($\text{Ru}^{3+}\text{-SO/Ru}^{3+}\text{-S}$) begins to appear, as well as E_{pa}^4 , corresponding to the oxidation of the unstable fully reduced form ($\text{Ru}^{2+}\text{-OS/Ru}^{2+}\text{-S}$). Figure 1c shows the behavior at 100 mV s^{-1} of the mononuclear species, ($\text{Ru}^{2+}\text{-SO/S}$). It is evident that this is very similar to Figure 1a when the contribution by the thioether-based couple is omitted.

In Figure 2, the values of $E_{1/2}$ for electrochemical steps 1 and 3 and of E_{pa} and E_{pc} for steps 2 and 4 at the 100 mV s^{-1} scan rate are shown, as well as, in parentheses, those obtained in the earlier work.⁴

By application of the double potential step method of Schwarz and Shain,⁸ the specific rates for the isomerizations of the metastable forms were determined and are entered in Table 1,

(10) (a) Bard, A. J.; Faulkner, L. R. *Electrochemical Methods, Fundamentals and Applications*; Wiley: New York, 1980; p 675. (b) Feldberg, S. W. *Electroanal. Chem. Interfacial Electrochem.* **1969**, 3, 199. (c) Magno, F.; Bontempelli, G.; Andreuzzi-Sedeia, M. *Anal. Chim. Acta* **1982**, 140, 65.

(8) Schwarz, W. M.; Shain, I. *J. Phys. Chem.* **1965**, 69, 30.

(9) Roush, P. B.; Musker, W. K. *J. Org. Chem.* **1978**, 43, 4295.

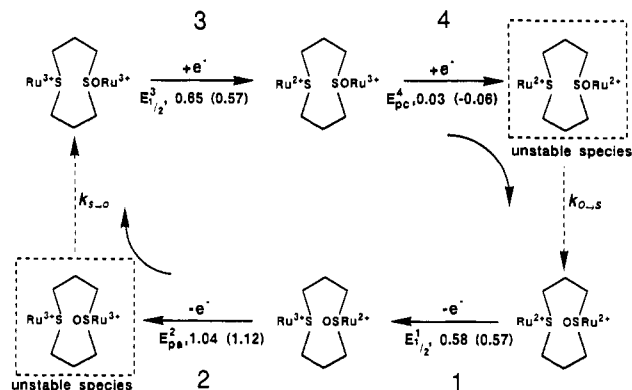


Figure 2. Redox behavior of the "molecular hysteresis" molecule at 100 mV s⁻¹. The values in parentheses are those reported in the earlier communication. The electrochemical steps are numbered.

Table 1. Redox Potentials for the Steps Leading to the Formation of the Metastable Products and Rate Constants for the Isomerization^a

	$E_{1/2}$, V	$k_{O \rightarrow S}$, s ⁻¹	$E_{1/2}$, V	$k_{S \rightarrow O}$, s ⁻¹
species 2	0.03	3.8 ± 0.6	1.04	13 ± 2
species 1	-0.04	12 ± 3	1.10	63 ± 1
[Ru(NH ₃) ₅ (DMSO)] ²⁺	0.07	14 ± 1	0.97	0.32 ± 0.01
[Ru(NH ₃) ₅ (DPSO)] ²⁺	0.13	<i>b</i>	1.12	33 ± 2

^a In acetone at 20 °C. ^b The Ru(III) species is unstable, and we were unable to obtain a reliable value.

which is devoted to the dynamics of the linkage isomerizations (also of the mononuclear species). The rate of isomerization of the fully oxidized metastable species, as reported earlier, is found to be greater than that of the fully reduced metastable species. The rates reported earlier, however, are a factor of 5 or so greater than the newer, more dependable values, a discrepancy somewhat larger than can be accommodated by any possible difference in temperature. The possibility of a calculational error in the earlier work is not excluded. The redox potentials recorded in Table 1 correspond to $E_{1/2}$ values for electrochemical steps 2 and 4 of the binuclear complex, each of which leads to a metastable product.

To test the validity of the treatment, the experimental trace shown in Figure 1a was simulated digitally. The appropriate data referred to in the paragraph above were used, diffusion was allowed for, and the rates of heterogeneous electron transfer were adjusted to give the best fit. The optimum values ($\pm 20\%$) of the dimensionless parameters^{10a} are as follows: $k_{sim}^0 = 0.04, 0.10, 0.17,$ and 0.08 for electrochemical steps 1–4. (To calculate real values of the heterogeneous rate constants, the diffusion coefficients of the electroactive species are needed, but these have not been determined.) The simulated trace, Figure 1d, corresponds quite closely to the experimental, indicating that the values of the kinetic parameters are reasonable.

Rate of Interconversion of the Mixed-Valence Species. In Figure 3 are shown the cyclic voltammograms at slow scan rates (20 mV s⁻¹) of the mononuclear species, 1, and the binuclear, 2 (traces a and b, respectively). The cathodic wave at $E \sim 0.0$ V is relatively more prominent for 1 than it is for the binuclear complex. Both signals are attenuated by diffusion of the electroactive species from the surface layer, but the comparison shows that an additional process comes into play for the binuclear. It is to be noted as well that the amplitude ratio of the anodic and cathodic scans of the reversible couple are scan rate dependent: the ratio of i_a/i_c at $E \sim 0.6$ V at the slow scan rate of 20 mV s⁻¹ is only 88% of that at 1 V s⁻¹.

To trace the source of the discrepancies noted, a program of digital simulation of the voltammogram of species 1 (scan rate 100 mV s⁻¹) was undertaken. The agreement with the experimental trace, Figure 1c, is very good. The simulation of the experimental data for species 2 at the scan rate of 100 mV s⁻¹

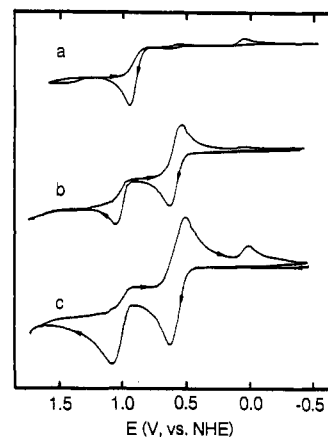


Figure 3. Cyclic voltammograms (in acetone at 20 °C; 0.10 M (*n*-Bu)₄PF₆ electroactive species at 1.0×10^{-3} M): (a) [Ru(NH₃)₅(SOS)]²⁺ at 20 mV s⁻¹; (b) [Ru(NH₃)₅(SOS)Ru(NH₃)₅]⁴⁺ at 20 mV s⁻¹; (c) [Ru(NH₃)₅(SOS)Ru(NH₃)₅]⁴⁺ at 50 mV s⁻¹.

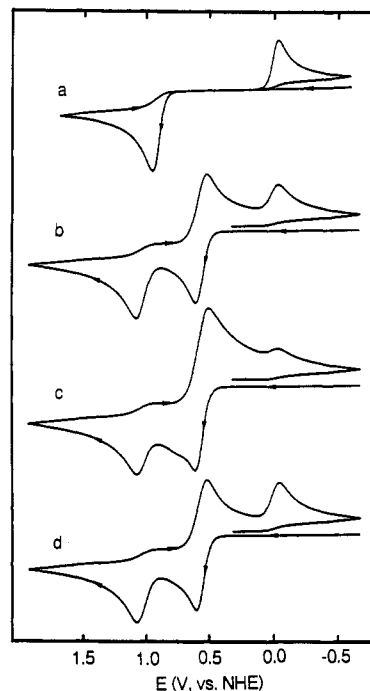
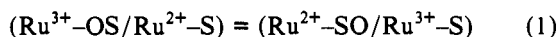


Figure 4. Digital simulations of cyclic voltammograms at 100 mV s⁻¹: (a) [Ru(NH₃)₅(SOS)]²⁺; (b) the best fitting result for [Ru(NH₃)₅(SOS)Ru(NH₃)₅]⁴⁺; (c) [Ru(NH₃)₅(SOS)Ru(NH₃)₅]⁴⁺ with a rapid intramolecular electronic transfer (1.2 s⁻¹); (d) [Ru(NH₃)₅(SOS)Ru(NH₃)₅]⁴⁺ with reverse intramolecular electron transfer at the same specific rate as for trace b.

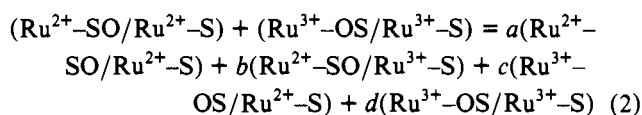
has already been referred to. The reduction wave at ~ 0.0 V for the experimental curve, Figure 1a, is smaller than that for the simulated, Figure 1d. We find that the discrepancy cannot be removed by adjusting the heterogeneous-charge-transfer rate constants nor can the difference in the amplitude ratios at 0.6 V mentioned above be accounted for by factors thus far considered. We conclude that discrepancies are due to loss of (Ru³⁺-OS/Ru²⁺-S) by a process in addition to diffusion, namely conversion of this species to (Ru²⁺-SO/Ru³⁺-S). Such conversion is in principle possible by both intra- and intermolecular electron transfer. Cyclic voltammetry scans made with the electroactive species 10-fold more dilute, other conditions remaining constant, eliminated the latter as contributing significantly at the concentration levels of our experiments.

Figure 4b shows the resulting digital simulation at 100 mV s⁻¹ made by now allowing also for intramolecular electron transfer shown in eq 1. The best fit was obtained by assuming k_f for this reaction to be $0.12 (\pm 0.04)$ s⁻¹, and the corresponding experimental

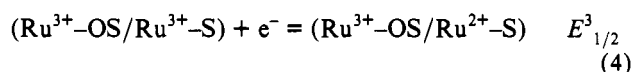
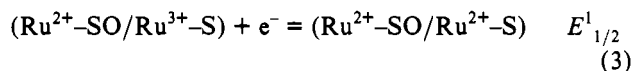


trace is shown in Figure 1a. There is a discrepancy between the simulated (Figure 4b) and the experimental trace (Figure 1a) at ca. 0.80 V, which we attribute to impurities. Figure 1c shows the result of assuming a value of k_f 10-fold greater. To be noted is that the feature at $E \cong 0.0$ V is now quite weak while the wave corresponding to the reduction at the thioether site is much enhanced. When, as for Figure 4d, it is assumed that $(\text{Ru}^{3+}\text{-OS/Ru}^{2+}\text{-S})$ is more stable than $(\text{Ru}^{2+}\text{-SO/Ru}^{3+}\text{-S})$, with intramolecular electron transfer also at 0.12 s^{-1} but in the reverse direction, the feature at $E \cong 0.0$ V is now too prominent.

To obtain the equilibrium quotient for the conversion of $(\text{Ru}^{3+}\text{-OS/Ru}^{2+}\text{-S})$ to $(\text{Ru}^{2+}\text{-SO/Ru}^{3+}\text{-S})$, a modified rotating-disk approach was used: the electroactive solution in the cell was stirred rapidly while a voltammogram was recorded (at a scan rate of 20 mV s^{-1}), which yielded information about the composition of the solution. This was made up of equal concentrations of the fully oxidized and fully reduced species and left at 20°C for more than 2 h to reach equilibrium. Equilibration leads to partial disappearance of the reactants and the appearance of two new species, as shown in (2). Conservation of charge



requires $2a + b + c = b + c + 2d$ or $a = d$. The ratio $[\text{Ru}^{2+}\text{-SO}]_{\text{tot}}/[\text{Ru}^{3+}\text{-OS}]_{\text{tot}}$ is given as $(a + b)/(c + d)$ and in duplicate experiments by use of the rotating disk electrode was determined as 1.86. An additional relation can be obtained by use of the redox potentials for the half-reactions



The corresponding values of $E_{1/2}$ were obtained by starting with the fully reduced and fully oxidized forms (prepared by bulk electrolysis) and in each case reversing the direction of the scan before the onset of the second electron-transfer step.

Reaction 4 subtracted from reaction 3 yields as constant for the equilibrium ratio $[(\text{Ru}^{2+}\text{-SO/Ru}^{2+}\text{-S})][(\text{Ru}^{3+}\text{-OS/Ru}^{3+}\text{-S})]/[(\text{Ru}^{2+}\text{-SO/Ru}^{3+}\text{-S})][(\text{Ru}^{3+}\text{-OS/Ru}^{2+}\text{-S})]$ ($=ad/bc$) the value 0.062. From the three relations, the equilibrium constant ($=b/c$) for reaction 1 was calculated as $2.2 (\pm 0.4)$ ($\Delta G^\circ = -1.9 \text{ kJ mol}^{-1}$). Since k_f for reaction 1 has been determined as 0.12 s^{-1} , $k_r = 0.055 \text{ s}^{-1}$.

The free energy differences for three sides of each of the subblocks being known, the remaining values governing the linkage isomerization steps are determined; the specific rates of spontaneous isomerization being known, those for the reverse reactions are also determined. The results on the dynamics of the "double-block" array are summarized in Figure 5.

The absorption spectra in the low-energy (500 nm to near-IR) range of the spectrum for the fully oxidized, the fully reduced, and the mixed-valence species were determined. For the fully oxidized, a band with a maximum at 452 nm is observed ($\epsilon = 540 \text{ M}^{-1} \text{ cm}^{-1}$) with no evidence of an additional band at longer wavelength. The fully reduced shows a maximum at 500 nm ($\epsilon = 22 \text{ M}^{-1} \text{ cm}^{-1}$). That for the mixed-valence forms was obtained by preparing a solution containing equal concentrations of the fully oxidized and the fully reduced and allowing 2 h for the solutions to equilibrate. The band maximum, which we assign

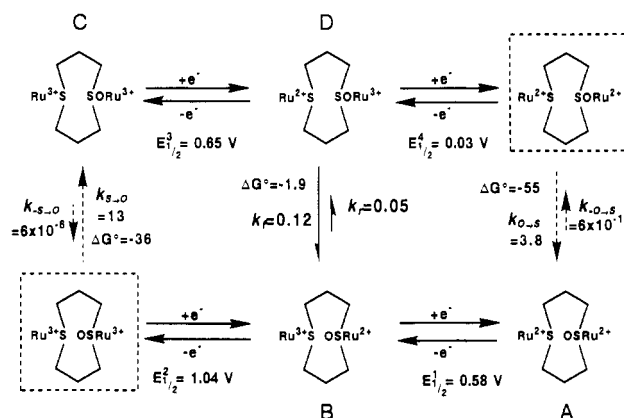


Figure 5. Equilibrium and rate parameters for the "Double-Block" reaction scheme.

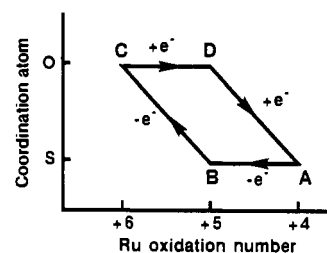


Figure 6. Schematic of the hysteresis behavior.

to the intervalence transition, is at 648 nm ($\epsilon = 37 \text{ M}^{-1} \text{ cm}^{-1}$ on the basis of the total concentration of the mixed-valence forms).

Discussion

The hysteresis behavior of the system is summarized in Figure 6, where switching from a mixed-valence state to the isomeric alternative is brought about by electron transfer. In applications, the speed at which these changes occur can be a critical factor. The responses in our system are slow, the rate being limited by the rate of conversion of the metastable, fully oxidized and fully reduced forms to the stable isomers. For the purpose of arriving at an understanding of the behavior of systems of this kind, the slow response is an advantage. Slow rates of substitution are typical of metal ions of the $\pi d^5/\pi d^6$ electronic structure type; by choice of metal centers with electronic structures which lead to greater substitution lability, the response times can be greatly shortened.

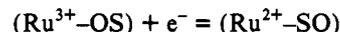
In our system, the interconversion of mixed-valence state **D** to mixed-valence state **B** by intramolecular electron transfer breaks the hysteresis loop, but there is no reason that, by suitable structural modifications, the electronic coupling on which electron transfer depends cannot be decreased to the point where it is not significant. For possible applications of molecules of this kind in high-density memory storage, and with light quanta being used to address the system, some electronic coupling is needed. Of special interest is the possibility of using frequencies in the range covered by the intervalence absorption to bring about the isomerization. We are confident, on the basis of the recent experiments, that we have observed an intervalence transition. In our system, because the redox potential for the reversible couple is close to the mean of $E_{1/2}^2$ and $E_{1/2}^4$, the equilibrium barrier to charge transfer within the two isomers is much the same, and if the Franck-Condon barriers are not much different, as seems likely, the intervalence bands for the two isomers will not be resolved. In such a case, at the light-induced steady state, the conversion of one isomer to another will be incomplete. However, by suitable choice of the potential of the reversible couple the overlap between the intervalence bands can be greatly reduced. Complete resolution is difficult because of the inherent breadth

of the transitions for valence-localized systems.¹¹ Other chromophores can also be introduced into molecules of this kind to bring about the photoconversion of one isomer of the mixed-valence species to another, a possibility that awaits future investigation. The mononuclear complex $[\text{Ru}(\text{NH}_3)_5(\text{DMSO})]^{2+}$ can also function as a switch, if linkage isomerism can be photoinduced. However, the lifetime of the unstable state can be short unless provision is made for electron transfer, which, as in the case of **2**, provides for "locking-in" the structural change.

As mentioned in our earlier paper,^{4a} the mixed-valence species of the kind with which we are dealing are of interest from a quite different perspective: they offer the opportunity to study basic aspects of the electron-transfer process for an important class of redox reagents in which the energy profile as a function of nuclear displacements shows a double minimum. Even the single result for a system of this kind has some points of interest. The driving force for the change from **D** to **B** is small, $-\Delta G^\circ = -1.9 \text{ kJ mol}^{-1}$. Electron transfer from Ru^{2+} to Ru^{3+} in **D** in the absence of linkage isomerism faces a barrier of ca. 0.62 V. Rearrangement of $\text{Ru}^{3+}\text{-OS}$ to $\text{Ru}^{3+}\text{-SO}$ takes place at a rate of $\sim 6 \times 10^{-6} \text{ s}^{-1}$ (see the conversion of **C** to the metastable isomer in Figure 5). It is evident that electron transfer in **D** does not await such a drastic change in structure prior to electron transfer. It is to be noted that when the reducing agents acts in the binuclear mode on a redox couple showing linkage isomerization on electron transfer, the rate of linkage isomerization controls the redox process. Thus, in the reaction of $[\text{Os}(\text{NH}_3)_5(\eta^2\text{-}(\text{CH}_3)_2\text{CO})]^{2+}$ with the oxidant $[\text{Os}(\text{NH}_3)_5(\text{PhCN})]^{3+}$,¹² the rate of reaction was found to be independent of the concentration of the oxidant in the range 0.9×10^{-3} to $5.9 \times 10^{-3} \text{ M}$. Evidently, the rate of oxidation of the η^2 -acetone complex is governed by the rate of spontaneous rearrangement to the η^1 form, and there is no significant contribution from the oxidant acting directly on the η^2 -acetone species, which would appear as a second-order rate term. In the binuclear mode, the reactant encounter time is indefinitely long, and electron transfer can proceed by a path in which the Franck-Condon restriction is met by vibrational distortions of the binuclear complex, without the necessity of waiting for the formation of an intermediate.

It is also worthy of note that the efficiency of electron transfer in the mixed-valence molecule in our system has provided a convenient means of closing the free energy cycle comprising the fully reduced and fully oxidized forms. The alternative bimolecular mode for measuring the rates of conversion of either of the stable forms to the metastable by scavenging the latter as it is formed¹² would have been difficult because of the low rates of

isomerization. Comparisons provided by the data in Table 1 show that, even in the present case, where the reversible couple is linked to the DMSO couple in a cyclic framework, which may place constraints on nuclear readjustments, the values of ΔG° for the DMSO couple are not greatly different from those observed for the mononuclear species. If it is assumed that the redox potential for the sulfoxide couple is only slightly perturbed by the inclusion of the reversible couple in the same molecule, an approximate value for the reduction potential governing the process



can be calculated. When this is done for the process in which the metal in the reversible couple is in the 2+ oxidation state, a value of 0.60 V is calculated, while, for the metal in the 3+ oxidation state, the value is 0.66 V.

Further work is being done on the dynamics of the sulfoxide linkage isomerizations, which includes measurement of rates as a function of temperature, and the present results will be commented on only briefly.¹³ The earlier work on the DMSO complex was done in water as solvent,⁶ and the behavior is complicated by aquation competing with rearrangement of the metastable forms. However, values of $k_{\text{S}\rightarrow\text{O}}$ (in the 3+ species) and $k_{\text{O}\rightarrow\text{S}}$ (in the 2+ species) are reported as $7.0 (\pm 0.5) \times 10^{-2}$ and $30 (\pm 7) \text{ s}^{-1}$, respectively, to be compared to 0.32 ± 0.01 and 14 ± 1 in acetone at somewhat lower temperature. The marked decline in $k_{\text{S}\rightarrow\text{O}}$ in water compared to acetone may be a consequence of the stronger interaction of the polar oxygen atom site in the hydrogen-bonding solvent. If this is in fact the cause of the rate difference, it suggests that in the 1,2 shift, bond making plays a significant role in the activation process, a not unreasonable possibility, considering the small distance separating the alternate sites.

Acknowledgment. We thank Professor W. K. Musker of the University of California (Davis) for a gift of 1,5-dithiacyclooctane, which we used in our first experiment. M.S. acknowledges Grant-in-Aid No. 03453048 for Scientific Research from the Ministry of Education, science, and Culture of Japan. M.S. also acknowledges the Presto-21 Project of the Japan Research Development Corp., Murata Foundation, Nihon Syoken Foundation, and Yazaki Foundation for support. H.T. acknowledges research supported by National Science Foundation Grant No. CHE-9120158-A01.

(11) Hush, N. S. *Prog. Inorg. Chem.* **1967**, *8*, 428 ff.

(12) Harman, W. D.; Sekine, M.; Taube, H. *J. Am. Chem. Soc.* **1988**, *110*, 2439.

(13) Tomita, A.; Sano, M. To be prepared.